Stem Cell Reports
Report
OPEN ACCESS

Enhanced Fitness of Adult Spermatogonial Stem Cells Bearing a Paternal Age-Associated FGFR2 Mutation

Laura A. Martin,[1] Nicholas Assif,[1] Moses Gilbert,[1] Dinali Wijewarnasuriya,[1] and Marco Seandel[1,*]
[1]Department of Surgery, Weill Cornell Medical College, New York, NY 10065, USA
*Correspondence: mseandel@med.cornell.edu
http://dx.doi.org/10.1016/j.stemcr.2014.06.007

SUMMARY

Pathogenic de novo mutations increase with fathers' age and could be amplified through competition between genetically distinct subpopulations of spermatogonial stem cells (SSCs). Here, we tested the fitness of SSCs bearing wild-type human FGFR2 or an Apert syndrome mutant, FGFR2 (S252W), to provide experimental evidence for SSC competition. The S252W allele conferred enhanced FGFR2-mediated signaling, particularly at very low concentrations of ligand, and also subtle changes in gene expression. Mutant SSCs exhibited improved competitiveness in vitro and increased stem cell activity in vivo upon transplantation. The fitness advantage in vitro only occurred in low concentrations of fibroblast growth factor (FGF), was independent of FGF-driven proliferation, and was accompanied by increased response to glial cell line-derived neurotrophic factor (GDNF). Our studies provide experimental evidence of enhanced stem cell fitness in SSCs bearing a paternal age-associated mutation. Our model will be useful for interrogating other candidate mutations in the future to reveal mechanisms of disease risk.

INTRODUCTION

Cell-to-cell competition among male germline stem cells has been proposed to account for the higher frequency of some disorders among children of older fathers, a correlation referred to as the paternal age effect (PAE) (Goriely and Wilkie, 2012). In addition to compelling observations in humans, evidence of male germline selection was noted in early mammalian models of genetic mosaicism (Jaenisch, 1976). However, the mechanism of positive selection for PAE mutations has not been directly interrogated in an experimental stem cell model.

Consistent with a role of germline selection, landmark studies correlated increasing numbers of pathogenic alleles with men's age either in sperm or in microanatomical clusters in the normal testis (Choi et al., 2008; Goriely et al., 2003). The observed rise in mutant allele frequency was above that which could be explained by alternate hypotheses (e.g., mutational hot spots) and was attributed to positive selection of mutant spermatogonial stem cells (SSCs), which represent the only long-lived germ cell in the mammalian testis. This provocative concept has been referred to as the selfish selection hypothesis (Goriely and Wilkie, 2012).

Several factors are crucial for SSC maintenance in mammals. Among these, glial cell line-derived neurotrophic factor (GDNF), secreted by Sertoli cells, binds to the RET/GFRα1 receptor complex, providing a critical signal for SSC survival (Meng et al., 2000). Seminal studies that established SSC culture conditions identified additional niche-derived growth factors (e.g., fibroblast growth factor [FGF] and epidermal growth factor [EGF]) that support maintenance of SSCs in vitro (Kubota et al., 2004). While genetic models determined that GDNF is essential, the effects of other growth factors in SSC fate decisions remain largely unclear.

Several signaling pathways and unique transcriptional programs are thought to control SSC self-renewal and differentiation in mammals. Transcriptional regulators typically associated with SSC self-renewal include *Plzf*, *Etv5*, *Bcl6b*, *Pou3f1*, *Lhx1*, and *Foxo1* (Buaas et al., 2004; Costoya et al., 2004; Goertz et al., 2011). GDNF induces *Etv5*, *Bcl6b*, and *Pou3f1* (Oatley et al., 2006). Etv5 and Foxo1 induce *Ret* expression, establishing a positive feedback mechanism for GDNF signaling to maintain self-renewal. FGF2 also increases the expression of *Etv5* through mitogen-activated protein kinase (MAPK) activation, contributing to SSC self-renewal, at least in part by increasing GDNF/RET signaling (Ishii et al., 2012). Additionally, activation of the AKT and MAPK signaling pathways by GDNF and FGF2 were correlated with SSC maintenance (Lee et al., 2007).

While SSC self-renewal requires growth factor signaling, previous studies have found that stem cell activity is impaired in the presence of excess FGF- or EGF-mediated signaling (Kubota et al., 2004). Moreover, excessive self-renewal signals induce oncogenic transformation and impair SSC maintenance (Goertz et al., 2011; Lee et al., 2009). In contrast, gain-of-function (GOF) mutations in fibroblast growth factor receptor 2 (FGFR2), associated with enhanced FGF signaling, are the basis for Apert syndrome, in which the PAE is particularly robust (Choi et al., 2008). Furthermore, other disorders that exhibit a strong PAE (e.g., achondroplasia and MEN2B) are due to mutant alleles that also increase growth factor signaling in affected organs and tissues (Goriely and Wilkie, 2012).

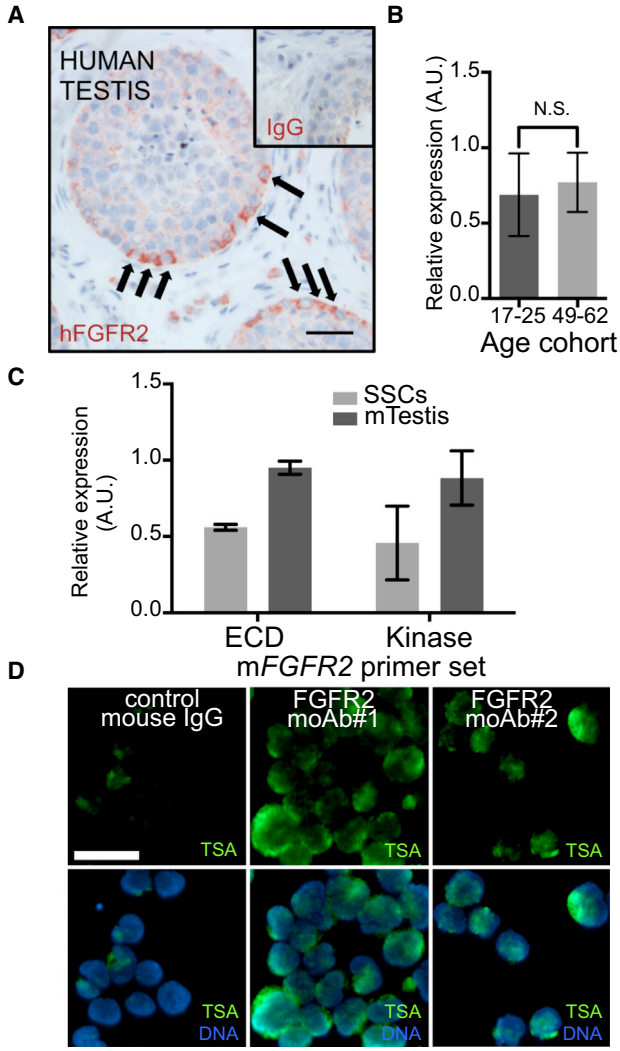

Figure 1. Expression of FGFR2 in Human Testis and in Mouse SSCs

(A) IHC with tyramide signal amplification (TSA) on adult human testis, showing positive reactivity (reddish brown; arrows) to monoclonal anti-human FGFR2 antibody exclusively in spermatogonia along the basement membrane (inset, mouse IgG; scale bar, 100 μm).

(B) qRT-PCR showing *FGFR2* expression levels in human testis from young (17–25 years; mean ± SD, n = 3 donors) and older (49–62 years; mean ± SD, n = 5 donors) cohorts.

(C) Relative *Fgfr2* expression in SSC lines compared to mouse testis (mTestis) using primers annealing in the extracellular (ECD) and the kinase domains, respectively (mean ± SD; n = 3 biological replicates).

(D) Immunostaining with TSA (green) in cultured mouse SSC cytospin preparations showing endogenous FGFR2 protein expression with two different monoclonal antibodies (moAb) (scale bar, 25 μm)

Hence, the selfish spermatogonial selection hypothesis presents a conundrum, since balanced signaling (i.e., through AKT and MAPK) seems necessary for SSC maintenance (Kanatsu-Shinohara and Shinohara, 2013). The aim of this study is to provide direct experimental evidence for the PAE mechanism in Apert syndrome and to reconcile how activating mutations could improve stem cell fitness. To this end, we constructed a model system with adult mouse SSCs. Both in long-term culture and upon transplantation into recipient mice, we demonstrate that a human Apert syndrome allele confers enhanced fitness to SSCs, concomitant with increased downstream signals that support self-renewal of SSCs.

RESULTS

Expression of FGFR2 in Human Testis and Adult Mouse SSCs

FGFR2 mutations (e.g., S252W) in Apert syndrome accumulate in the testes of older men (Goriely et al., 2003). However, previous studies did not establish FGFR2 protein distribution in spermatogonia. When we attempted to localize FGFR2 using conventional immunostaining, no signal was observed (data not shown). Then, by using the highly sensitive tyramide signal amplification (TSA) approach, anti-FGFR2 monoclonal immunoreactivity was detected adjacent to the basement membrane in the human testis, consistent with the known location of spermatogonia. No reactivity was observed in differentiated germ cells or Sertoli cells (Figure 1A). We next evaluated the expression of FGFR2 in the human testis by quantitative RT-PCR (qRT-PCR). FGFR2 was detected at the mRNA level in samples of normal adult human testis across a wide age range (17–62 years; Figure 1B).

To confirm that mouse SSCs represent a good model in which to address the PAE mechanism in Apert syndrome, SSCs in long-term culture were tested for FGFR2 expression. We had previously derived primary SSC lines from adult mice and confirmed their stem cell activity in vivo (Martin and Seandel, 2013; Seandel et al., 2007). Expression of FGFR2 was found by both qRT-PCR and immunofluorescence (IF) with TSA in several independently derived SSC lines (Figures 1C and 1D). Taken together, these data suggest that FGFR2 is normally expressed in the mammalian testis, albeit at low levels, in cell populations that could propagate a long-term clonal effect. Based on this, we used mouse SSC lines to address the cellular mechanism of the FGFR2-mediated PAE.

Ectopic Expression of hFGFR2 Alleles in Mouse SSCs

To test the selfish selection hypothesis experimentally and assess fitness of wild-type (WT) versus mutant SSCs, we

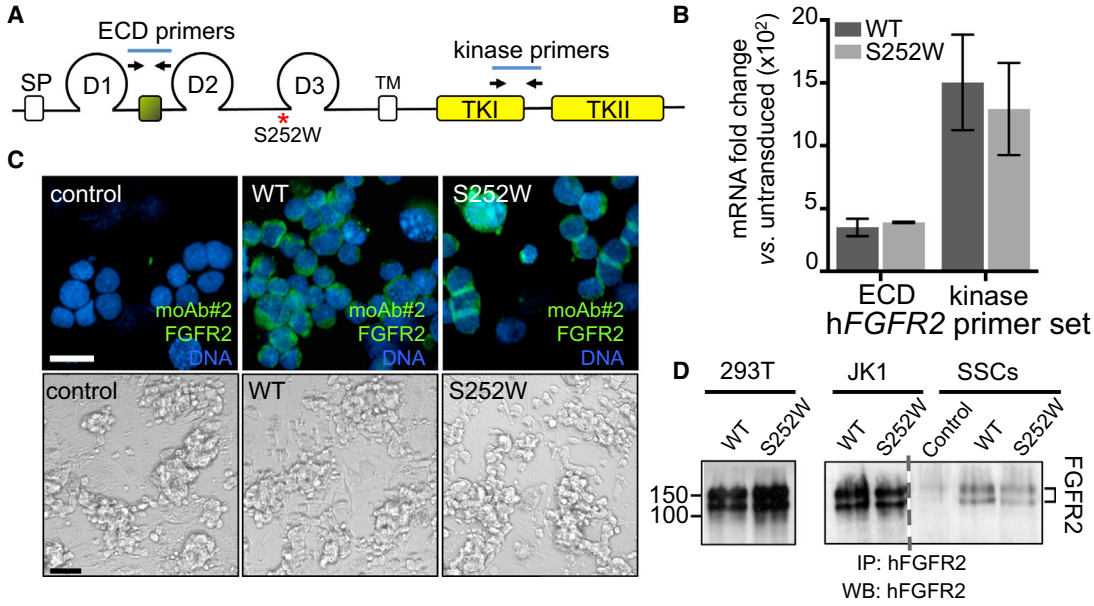

Figure 2. Delivery of Ectopic Human FGFR2 Alleles in Adult Mouse SSCs

(A) Schematic of FGFR2 protein and primers for human-specific *FGFR2* qRT-PCR. Asterisk marks the location of the S252W Apert mutation (ECD, extracellular domain).

(B) qRT-PCR using two sets of primers showing relative expression levels of hFGFR2 in lentivirus-transduced SSCs bearing WT hFGFR2 (WT) or human S252W FGFR2 (S252W) with untransduced SSCs as the reference control (mean ± SD of three independent cell lines per genotype).

(C) IF on cytospins (top row) with anti-hFGFR2 antibody (green) for SSCs stably expressing WT (middle) or S252W (right) alleles and untransduced SSCs as control (left). Scale bar, 10 μm. Phase contrast (bottom row) of untransduced SSCs (control; left) or stably expressing hFGFR2 WT (middle) or S252W (right) alleles in standard culture conditions (scale bar, 50 μm).

(D) Immunoprecipitation (IP) and detection with two specific monoclonal antibodies for hFGFR2 in WT and S252W SSC. Controls: untransduced SSCs and JK1 feeder cells or 293T cells transduced with WT or S252W lentiviruses. Grey dashed line denotes cropped lane. See also Figure S1.

generated adult mouse SSCs stably expressing WT human FGFR2 or the PAE-associated FGFR2 S252W Apert syndrome mutation (referred to as WT or S252W hFGFR2 hereafter) by transduction with lentiviruses. Expression levels of hFGFR2 in each SSC line were measured by qRT-PCR with specific primers for the human gene (Figures 2A and 2B). Human FGFR2 protein expression in SSCs was compared by IF and immunoprecipitation followed by immunoblot (IB) with monoclonal antibodies that specifically recognize hFGFR2, confirming similar expression levels for both hFGFR2 alleles and equivalent cellular distribution (Figures 2C and 2D).

Potential mechanisms that would result in a selective advantage to different clonal cell populations within a given environment include enhanced proliferative capacity or survival. We compared each of these parameters in WT and S252W SSCs by measuring expansion of cell populations over time, mitotic fraction, apoptosis, and also cell adhesion. No significant differences were found between the two cell populations (Figures S1A–S1D available online). Next, we asked whether alterations in the frequency of asymmetric (*i.e.*, differentiating) cell divisions could change the ratio of WT versus mutant spermatogonia. As a surrogate for differentiation capacity, we tested the response of WT and mutant SSCs to retinoic acid (RA), shown previously to initiate spermatogonial differentiation in vitro in a physiologically relevant manner (Dann et al., 2008). Both cell populations responded appropriately to RA exposure by upregulating genes associated with differentiation and downregulating stem cell-associated genes (Figure S1E). To determine whether the stem cell phenotype per se could mediate the PAE observed in Apert syndrome, we surveyed expression levels of genes associated with self-renewal and differentiation in WT versus S252W SSCs (Figures S1F–S1H). Although consistent differences in expression of most genes were not seen, we did find markedly higher expression of *Etv5*, a critical transcription factor for SSC maintenance, in S252W SSCs (Oatley et al., 2006).

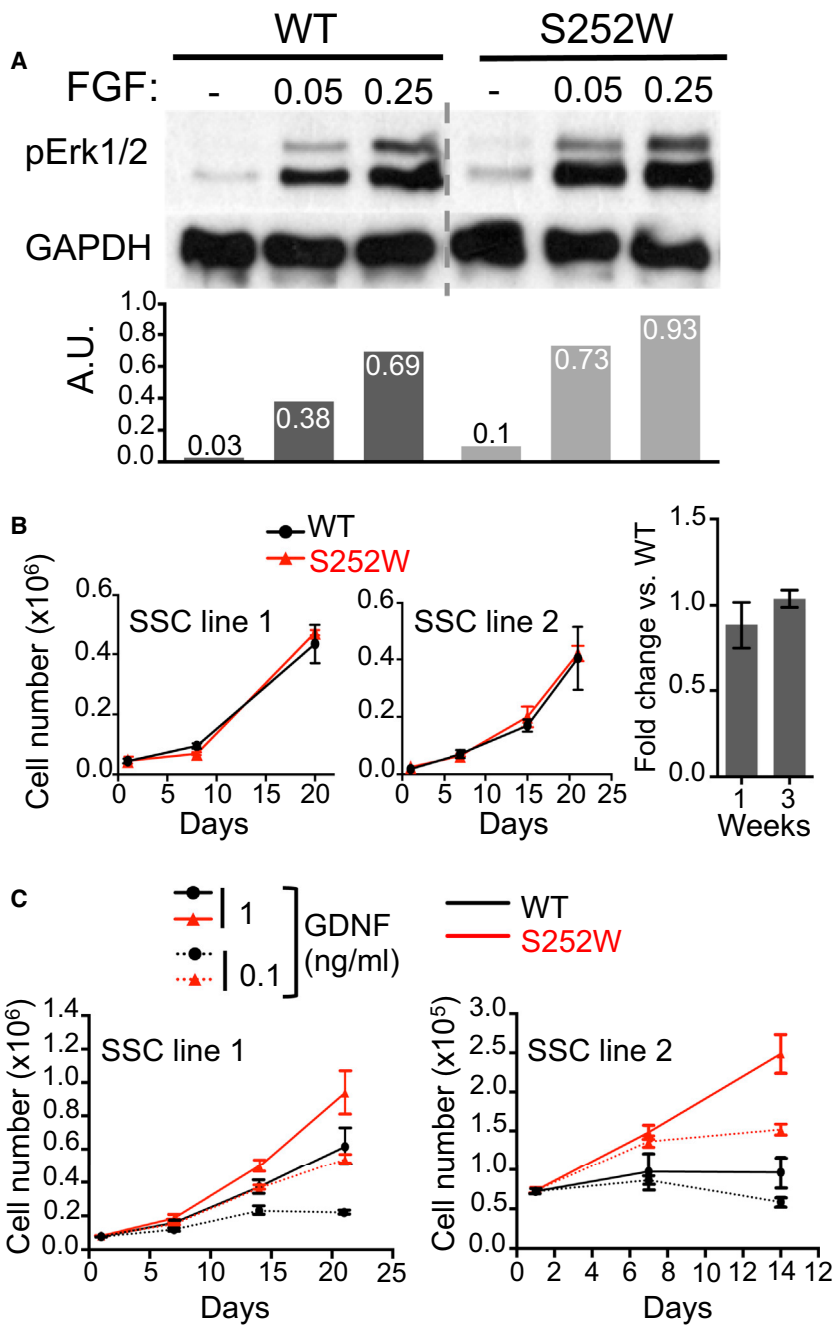

Figure 3. Enhanced Sensitivity of S252W SSCs to FGF

(A) Representative anti-p42/44 MAPK (pErk1/2) IB in WT and S252W SSCs in response to FGF2 doses (0.05 and 0.25 ng/ml). Grey dashed line denotes cropped lane. Graphs correspond to densitometric analyses of IB image above for pErk1/2, normalized to loading control (GADPH), with values shown for each condition in arbitrary units (A.U.).

(B and C) Proliferation curves showing WT and S252W SSC numbers (mean ± SD; n = 3 wells/condition) after 2–4 weeks in vitro with either (B) reduced FGF2 (1 ng/ml) or (C) reduced GDNF (doses shown) and reduced FGF2 (1 ng/ml). Curves correspond to two biological replicates. Bar graph in (B) depicts fold change in total cell number of S252W versus WT SSCs at indicated time points in three biological replicates (mean ± SD).

See also Figure S2.

S252W SSCs Exhibit Enhanced Sensitivity to Growth Factors

Our preliminary characterization of the hFGFR2 SSC lines suggested a mechanism of autonomously increased self-renewal potential of S252W SSCs. However, relatively little is known about how FGFR2-mediated signaling affects SSC self-renewal. Previous studies in other cellular contexts have demonstrated that the S252W FGFR2 mutant receptor exhibits decreased ligand dissociation (Anderson et al., 1998). Accordingly, we compared pMAPK and also pAKT levels in WT and S252W SSCs upon FGF2 stimulation. While no consistent differences were detected at ≥0.5 ng/ml FGF2 (data not shown), S252W SSCs yielded greater pMAPK and, to a more moderate extent, greater pAKT at lower FGF2 concentrations than WT cells (Figures 3A and S2A). Notably, in the presence of reduced FGF2 (1 ng/ml), there was no difference in the proliferation of the two cell variants (Figure 3B).

Based on our observations with hFGFR2 SSCs, we interrogated the effect of FGF dose on downstream signaling

through endogenous FGF receptors. Low doses of FGF2 induced pMAPK and pAKT and loss of pStat3 (Figures S2B–S2D). However, higher doses of FGF2 reversed this effect. In contrast, GDNF induced a dose-dependent increase in pMAPK and pAKT (Figures S2E and S2F). To test the sustained effects FGF2, we profiled SSCs at varying chronic doses (0–10 ng/ml) and found an inverse relationship of FGF dose and expression levels for certain stem cell markers (*i.e.*, *Id4*, *Etv5*, and *Sall4*), while other markers (*Ret*, *Pou3F1*, *Lhx1*, and *Kit*) did not change (Figures S2G and S2I). These data are generally concordant with a previous study using a different culture system, which showed that SSCs maintained at a relatively low FGF2 dose exhibit higher colonization activity, compared to SSCs cultured with higher doses of FGF2 (Kubota et al., 2004).

Based on the increased responsiveness of S252W SSCs to FGF (Figures 3A and S2A), we asked next whether enhanced FGFR2 signaling could alleviate the requirement for GDNF. To test this possibility, WT and S252W SSCs were cultured in reduced FGF2 and GDNF concentrations. Compared to WT SSCs, S252W SSCs exhibited increased cell recovery under these conditions and were able to overcome a substandard GDNF concentration (Figure 3C). Collectively, these results suggest that the Apert S252W mutation enables SSCs to withstand the potentially detrimental effects of reduced growth factors in the niche.

Competition between WT and S252W SSCs

Our data above suggest an increased self-renewal capability of S252W SSCs, particularly when growth factors are limited. However, the selfish selection hypothesis proposes a competition-based mechanism (Goriely and Wilkie, 2012). Thus, we asked next whether the Apert S252W mutation confers higher functional stem cell activity and a selective advantage that enables mutants to outcompete WT counterparts. To this end, differentially labeled WT and S252W SSCs expressing GFP or mCherry, respectively, were cocultured in vitro for several weeks or mixed immediately prior transplantation as shown in Figure 4A.

For in vitro evaluation, differentially labeled populations were mixed in the presence of varying FGF concentrations to impose a selective pressure. Changes in the S252W-to-WT ratio were measured serially by flow cytometry (fluorescence-activated cell sorting [FACS]; Figures 4B and S3C, and S3D). After several weeks of coculture, S252W-expressing SSCs progressively outcompeted WT cells independently of the initial mixing ratio and became the predominant population in the culture. Of note, this difference was only observed in the presence of reduced FGF conditions, but not in standard culture media (Figures 4B and S3A).

We next assessed stem cell activity of cultured WT and S252W SSCs in vivo by transplantation into busulfan-treated mice. Differentially labeled WT and S252W SSCs were mixed immediately prior to transplantation into the testis. GFP^+ and $mCherry^+$ colonies were counted 2 months after surgery, revealing that mutant cells exhibited significantly greater stem cell activity than WT (Figure 4C). Similar results were obtained when GFP and mCherry labels were reversed, excluding intrinsic effects of the labeling system. In an alternate experimental design, the two populations were mixed and cocultured in vitro for several weeks prior to transplantation with similar results (data not shown). Collectively, these data demonstrate that the S252W PAE mutation confers a fitness advantage to SSCs.

DISCUSSION

The selfish spermatogonia selection hypothesis proposes that pathogenic alleles in human PAE disorders become enriched through clonal expansion of mutant SSCs that possess an acquired competitive advantage (Goriely and Wilkie, 2012). Here, we modeled stem cell fitness prospectively to address the effects of a PAE-associated hFGFR2 mutation in adult SSCs. In vitro cell competition data together with cotransplantation constitute the only experimental evidence to date for increased fitness and stem cell activity of mutant S252W SSCs over WT.

Cell competition in adults plays a role in organ homeostasis; for example, germline stem cells in *Drosophila* continuously compete for niche occupancy (Zhao and Xi, 2010). To some extent, stem cell replacement occurs in a stochastic manner (Klein et al., 2010). However, sporadically occurring mutations during aging or certain pathological processes (e.g., cancer) can influence stem cell dynamics. The competitive advantage of tumor cell subclones provides a compelling analogy for the PAE mechanism proposed here and elsewhere (Goriely and Wilkie, 2012). Even so, several features differ. First, tumor cells do not retain their full differentiation capacity or functionality as differentiated cells. Our data show that mutant SSCs are capable of responding to RA similar to WT cells in vitro, suggesting that early differentiation is unaffected. Also, our studies did not detect marked differences in FGF-mediated proliferation or survival of SSCs in vitro, even under media conditions in which a competitive advantage was observable. On the other hand, mutant cells exhibit increased expression of *Etv5*, a critical transcription factor to maintain SSCs, implying some level of intrinsically elevated self-renewal capability of mutant cells over WT.

Also intriguing is the minimal overlap between the spectrum of acquired mutations in the most common forms of testicular cancer and the congenital variants observed in PAE disorders. In addition to Apert syndrome alleles, other pathogenic mutations, including those in RET and PTPN11, exhibit both a strong PAE and evidence of clonal

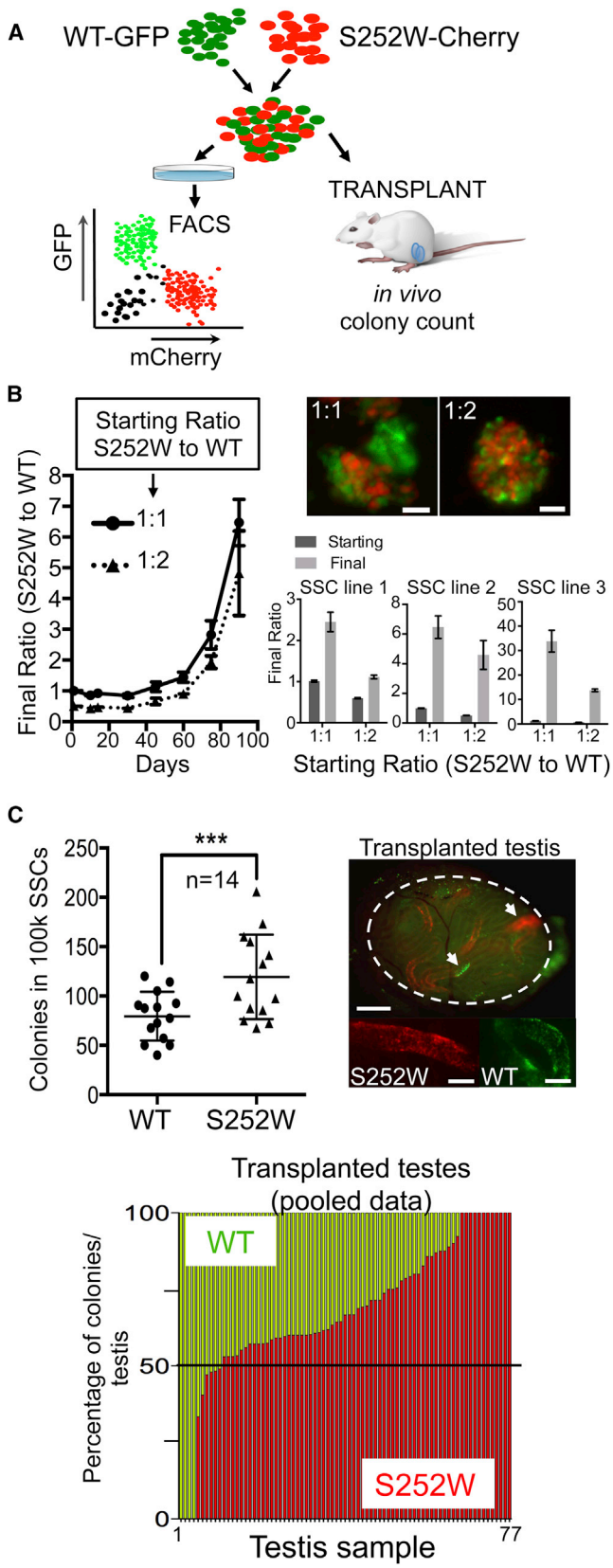

Figure 4. Enhanced Stem Cell Fitness of S252W SSCs

(A) Schematic of mixing experiments to assess fitness of WT versus S252W SSCs. For in vitro experiments, differentially labeled WT and mutant SSCs were mixed and cultured with different doses of FGF2. Stem cell activity was measured by transplantation into busulfan-treated mice. Two months after transplantation, the number of GFP and mCherry colonies in each testis was counted.

(B) In vitro mixing experiment showing a significant change over time in the ratio (FACS) of cocultured S252W and WT SSCs in reduced FGF2 (1 ng/ml), for both 1:1 and 1:2 starting ratios. Curves correspond to one representative biological replicate and show the mean (±SD; n = 3 wells/time point). Fluorescent images show mixed SSC colonies (scale bar, 50 μm). Bar graphs show the starting (i.e., measured postplating) and final ratios in three biological replicates. Error bars correspond to ±SD; n = 3 wells/time point.

(C) Top: representative transplantation experiment showing colony quantification for each genotype in transplanted testes (n = 14) with mixed WT-GFP and S252W-mCherry SSCs. ***p < 0.005 (Wilcoxon matched-pairs signed rank test). Fluorescent images: a transplanted testis with WT (green) and mutant (red) colonies (arrows; dashed line denotes testis border; scale bar, 1 mm) (top image), and representative WT (green) and S252W (red) colony detail (scale bars, 200 μm) (bottom images). Bottom: pooled transplant data (n = 10 experiments, 77 testes) showing the normalized percentage of colonies of each genotype per testis. See also Figure S3.

expansion of SSCs (Yoon et al., 2013). However, most PAE mutations documented to date are weakly acting, consistent with the idea that excessive upstream signal is deleterious to self-renewal. Indeed, we found diminished pMAPK and pAKT but increased pSTAT3 when SSCs were exposed to high FGF2. This finding also fits with the decreased SSC colonization observed when SSC are cultured in higher FGF or EGF doses (Kubota et al., 2004). Accordingly, S252W SSCs exhibited increased sensitivity to low FGF2 doses, as evidenced by slightly enhanced downstream signaling (i.e., through MAPK and AKT), compared to WT SSCs. Taken together, these data could provide a further explanation for why only mild GOF mutations are typically found in congenital disorders, as opposed to strongly activating somatic mutations in tumorigenesis.

Enhanced downstream signaling could confer resistance to a suboptimal niche. Strikingly, a recent study in a model of intestinal tumorigenesis showed that stem cells bearing activating mutations only acquired an advantage in a deteriorated niche (Vermeulen et al., 2013). In fact, we observed an in vitro advantage for mutants in low FGF2 conditions only. However, the finding that mutant SSCs grown in standard, high growth factor media still exhibited higher stem cell activity at transplant suggests that the FACS-based metric of fitness in vitro may be less sensitive than the transplant-based readout. Also, it is certain that the culture milieu does not perfectly recapitulate the stem cell niche in vivo. Unexpectedly, our data also show that mutant

SSCs can be maintained even when GDNF is limiting. Finally, previous studies revealed decreased expression of critical SSC growth factors, such as GDNF and FGF2, during normal aging and an age-related decline in niche function (Ryu et al., 2006). Taken together, these findings suggest that niche-dependent signaling in the mammalian testis must undergo exquisite regulation to avoid stem cell loss. Therefore, slight changes in the microenvironment could have profound effects on cell phenotype, such that otherwise neutral genotypes become beneficial under stressful conditions or with aging.

Other cell-extrinsic mechanisms may lead to a progressive loss of WT cells through an active process that eliminates the least fit populations. Such processes occur during normal development in the mammalian embryo, in which relatively unfit populations are deleted through apoptosis (Clavería et al., 2013). At present, we cannot exclude the possibility that active elimination of WT cells contributes to selection of FGFR2 S252W mutants. Perhaps the degree of PAE observed in different disorders reflects diverse mechanisms of stem cell competition occurring in the testis.

While the association between paternal age and risk monogenic disorders was observed >100 years ago, a variety of recent evidence has implicated de novo mutations in complex disorders, such as autism and schizophrenia (Goriely and Wilkie, 2012). We speculate that a subset of such mutations become enriched by a similar mechanism as in Apert syndrome. Therefore, in a society of increasingly older fathers, a relatively large swath of disease risk could originate in SSCs, even if the absolute increase in risk due to paternal age for any one disorder is low (Martin et al., 2010). For these reasons, it will be essential to more thoroughly elucidate the common mechanisms (or divergent pathways) that lead to SSC competition in subsequent studies.

EXPERIMENTAL PROCEDURES

SSC Culture

SSC lines were derived from C57Bl6/129S adult mice and maintained on mitotically inactivated JK1 feeder cells as previously described (Martin and Seandel, 2013). StemPro-34 containing 20 ng/ml GDNF, 10 ng/ml FGF2, 20 ng/ml EGF, and 25 μg/ml insulin was used for SSC culture (Seandel et al., 2007). SSC lines stably expressing hFGFR2 alleles and GFP or mCherry were generated by lentivirus. Feeder-free SSCs were treated with 1 μM RA or vehicle control for 72 hr (Dann et al., 2008). For cytokine stimulation, feeder-free SSCs were starved overnight and stimulated for 20 min with growth factors. Experiments were performed at least twice using SSC lines derived from different mice. For in vitro competition, mixed, differentially labeled WT and S252W SSCs were plated in triplicate and cocultured for several weeks in FGF2 (0.2–10 ng/ml). The mutant-to-WT ratio was determined serially by FACS (Accuri C6). All mouse experiments were performed in accordance with institutional and national guidelines and regulations including the Weill Cornell Medical College Institutional Animal Care and Use Committee.

SSC Transplantation

SSC transplant assays were performed as described previously using busulfan-conditioned mice (Seandel et al., 2007). Differentially labeled WT and S252W SSCs were mixed immediately prior to transplantation or first cocultured in vitro for several weeks. Two months later, detunicated recipient testes were analyzed for GFP^+ or $mCherry^+$ colonies and quantified using a fluorescent stereoscope (Zeiss).

Immunodetection

Human cadaver testis tissue was obtained from the New York Organ Donor Network (Sachs et al., 2014). Whereas IHC for endogenous FGFR2 in human tissue and SSC lines required TSA, detection of ectopic human FGFR2 was performed using standard biotin-conjugated secondary antibodies and streptavidin-fluorophore conjugates as detailed in the Supplemental Experimental Procedures. FGFR2 was detected using two different monoclonal anti-human FGFR2 antibodies (ab119237, Abcam; and sc-6930, Santa Cruz Biotechnology). Phospho-histone 3 serine10 (PH3) was detected with anti-PH3 (Millipore 06-570). Immunoprecipitation was performed using protein lysates from feeder-free SSCs and anti-human FGFR2 rabbit monoclonal antibody (D4H9, Cell Signaling). Immunoblot was performed with anti-human FGFR2 antibody (ab119237, Abcam). Detailed methods are found in the Supplemental Experimental Procedures.

For more information, please refer to Supplemental Experimental Procedures.

SUPPLEMENTAL INFORMATION

Supplemental Information includes Supplemental Experimental Procedures and three figures and can be found with this article online at http://dx.doi.org/10.1016/j.stemcr.2014.06.007.

ACKNOWLEDGMENTS

Supported in part by grant 5-FY11-571 from the March of Dimes Foundation (to M.S.), New York State Department of Health grant C026878 (to L.M.), and NIH grant 1DP2HD080352-01 (to M.S.). We thank Jun Zhang, Ph.D., for help with gene cloning and Todd Evans, Ph.D., and Shahin Rafii, M.D., for critical input.

Received: February 24, 2014
Revised: June 18, 2014
Accepted: June 20, 2014
Published: July 17, 2014

REFERENCES

Anderson, J., Burns, H.D., Enriquez-Harris, P., Wilkie, A.O., and Heath, J.K. (1998). Apert syndrome mutations in fibroblast growth factor receptor 2 exhibit increased affinity for FGF ligand. Hum. Mol. Genet. *7*, 1475–1483.

Buaas, F.W., Kirsh, A.L., Sharma, M., McLean, D.J., Morris, J.L., Griswold, M.D., de Rooij, D.G., and Braun, R.E. (2004). Plzf is required in adult male germ cells for stem cell self-renewal. Nat. Genet. *36*, 647–652.

Choi, S.K., Yoon, S.R., Calabrese, P., and Arnheim, N. (2008). A germ-line-selective advantage rather than an increased mutation rate can explain some unexpectedly common human disease mutations. Proc. Natl. Acad. Sci. USA *105*, 10143–10148.

Clavería, C., Giovinazzo, G., Sierra, R., and Torres, M. (2013). Myc-driven endogenous cell competition in the early mammalian embryo. Nature *500*, 39–44.

Costoya, J.A., Hobbs, R.M., Barna, M., Cattoretti, G., Manova, K., Sukhwani, M., Orwig, K.E., Wolgemuth, D.J., and Pandolfi, P.P. (2004). Essential role of Plzf in maintenance of spermatogonial stem cells. Nat. Genet. *36*, 653–659.

Dann, C.T., Alvarado, A.L., Molyneux, L.A., Denard, B.S., Garbers, D.L., and Porteus, M.H. (2008). Spermatogonial stem cell self-renewal requires OCT4, a factor downregulated during retinoic acid-induced differentiation. Stem Cells *26*, 2928–2937.

Goertz, M.J., Wu, Z., Gallardo, T.D., Hamra, F.K., and Castrillon, D.H. (2011). Foxo1 is required in mouse spermatogonial stem cells for their maintenance and the initiation of spermatogenesis. J. Clin. Invest. *121*, 3456–3466.

Goriely, A., and Wilkie, A.O. (2012). Paternal age effect mutations and selfish spermatogonial selection: causes and consequences for human disease. Am. J. Hum. Genet. *90*, 175–200.

Goriely, A., McVean, G.A., Röjmyr, M., Ingemarsson, B., and Wilkie, A.O. (2003). Evidence for selective advantage of pathogenic FGFR2 mutations in the male germ line. Science *301*, 643–646.

Ishii, K., Kanatsu-Shinohara, M., Toyokuni, S., and Shinohara, T. (2012). FGF2 mediates mouse spermatogonial stem cell self-renewal via upregulation of Etv5 and Bcl6b through MAP2K1 activation. Development *139*, 1734–1743.

Jaenisch, R. (1976). Germ line integration and Mendelian transmission of the exogenous Moloney leukemia virus. Proc. Natl. Acad. Sci. USA *73*, 1260–1264.

Kanatsu-Shinohara, M., and Shinohara, T. (2013). Spermatogonial stem cell self-renewal and development. Annu. Rev. Cell Dev. Biol. *29*, 163–187.

Klein, A.M., Nakagawa, T., Ichikawa, R., Yoshida, S., and Simons, B.D. (2010). Mouse germ line stem cells undergo rapid and stochastic turnover. Cell Stem Cell *7*, 214–224.

Kubota, H., Avarbock, M.R., and Brinster, R.L. (2004). Culture conditions and single growth factors affect fate determination of mouse spermatogonial stem cells. Biol. Reprod. *71*, 722–731.

Lee, J., Kanatsu-Shinohara, M., Inoue, K., Ogonuki, N., Miki, H., Toyokuni, S., Kimura, T., Nakano, T., Ogura, A., and Shinohara, T. (2007). Akt mediates self-renewal division of mouse spermatogonial stem cells. Development *134*, 1853–1859.

Lee, J., Kanatsu-Shinohara, M., Morimoto, H., Kazuki, Y., Takashima, S., Oshimura, M., Toyokuni, S., and Shinohara, T. (2009). Genetic reconstruction of mouse spermatogonial stem cell self-renewal in vitro by Ras-cyclin D2 activation. Cell Stem Cell *5*, 76–86.

Martin, L.A., and Seandel, M. (2013). Serial enrichment of spermatogonial stem and progenitor cells (SSCs) in culture for derivation of long-term adult mouse SSC lines. J. Vis. Exp. *72*, e50017.

Martin, J.A., Hamilton, B.E., Sutton, P.D., Ventura, S.J., Mathews, T.J., Kirmeyer, S., and Osterman, M.J. (2010). Births: final data for 2007. Natl. Vital Stat. Rep. *58*, 1–85.

Meng, X., Lindahl, M., Hyvönen, M.E., Parvinen, M., de Rooij, D.G., Hess, M.W., Raatikainen-Ahokas, A., Sainio, K., Rauvala, H., Lakso, M., et al. (2000). Regulation of cell fate decision of undifferentiated spermatogonia by GDNF. Science *287*, 1489–1493.

Oatley, J.M., Avarbock, M.R., Telaranta, A.I., Fearon, D.T., and Brinster, R.L. (2006). Identifying genes important for spermatogonial stem cell self-renewal and survival. Proc. Natl. Acad. Sci. USA *103*, 9524–9529.

Ryu, B.Y., Orwig, K.E., Oatley, J.M., Avarbock, M.R., and Brinster, R.L. (2006). Effects of aging and niche microenvironment on spermatogonial stem cell self-renewal. Stem Cells *24*, 1505–1511.

Sachs, C., Robinson, B.D., Andres Martin, L., Webster, T., Gilbert, M., Lo, H.-Y., Rafii, S., Ng, C.K., and Seandel, M. (2014). Evaluation of candidate spermatogonial markers ID4 and GPR125 in testes of adult human cadaveric organ donors. Andrology *2*, 607–614.

Seandel, M., James, D., Shmelkov, S.V., Falciatori, I., Kim, J., Chavala, S., Scherr, D.S., Zhang, F., Torres, R., Gale, N.W., et al. (2007). Generation of functional multipotent adult stem cells from GPR125+ germline progenitors. Nature *449*, 346–350.

Vermeulen, L., Morrissey, E., van der Heijden, M., Nicholson, A.M., Sottoriva, A., Buczacki, S., Kemp, R., Tavaré, S., and Winton, D.J. (2013). Defining stem cell dynamics in models of intestinal tumor initiation. Science *342*, 995–998.

Yoon, S.R., Choi, S.K., Eboreime, J., Gelb, B.D., Calabrese, P., and Arnheim, N. (2013). Age-dependent germline mosaicism of the most common noonan syndrome mutation shows the signature of germline selection. Am. J. Hum. Genet. *92*, 917–926.

Zhao, R., and Xi, R. (2010). Stem cell competition for niche occupancy: emerging themes and mechanisms. Stem Cell Rev. *6*, 345–350.

Stem Cell Reports, Volume *3*

Supplemental Information

Enhanced Fitness of Adult Spermatogonial Stem Cells Bearing a Paternal Age-Associated FGFR2 Mutation

Laura A. Martin, Nicholas Assif, Moses Gilbert, Dinali Wijewarnasuriya, and Marco Seandel

Figure S1

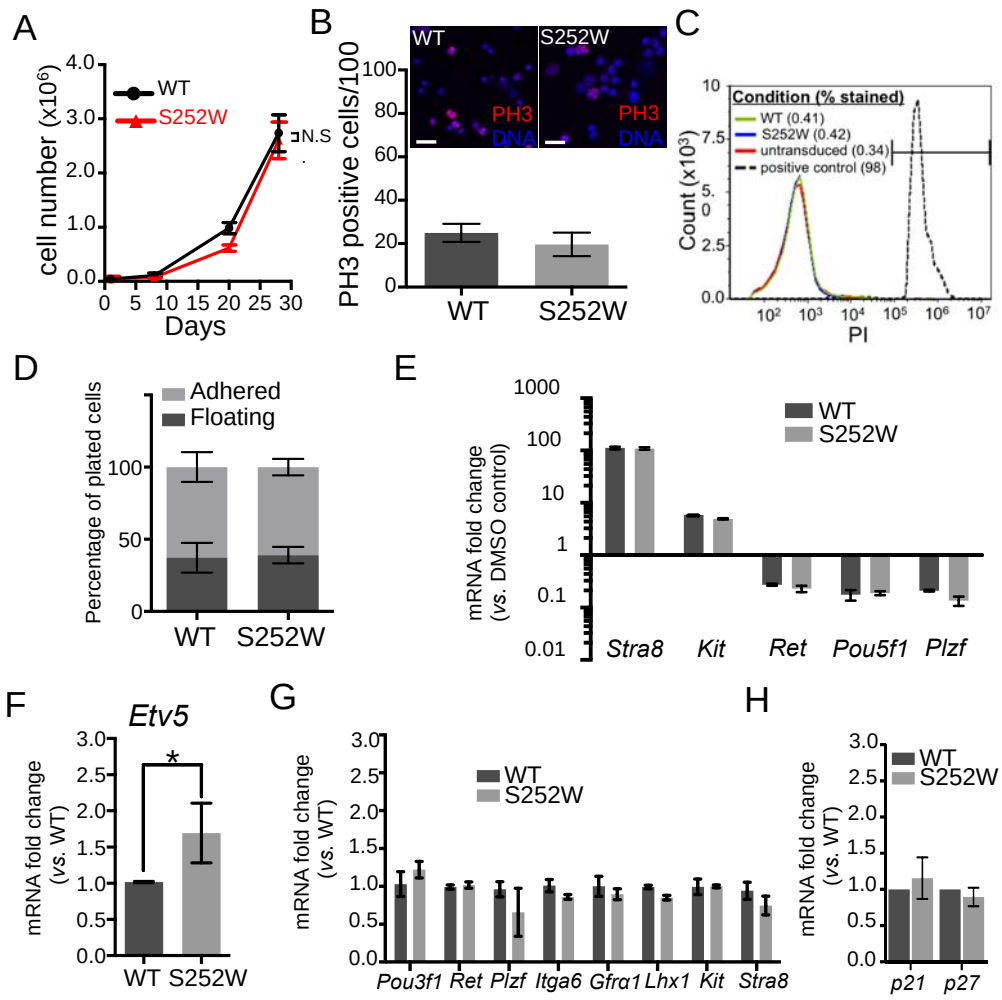

Figure S1, Related to Figure 2. Comparison of Phenotype in WT and S252W SSCs **(**A) Growth curves of WT and S252W SSCs after several weeks *in vitro* in standard culture conditions. Data represent mean ± SD; n=3 wells per time point). N.S., p >0.05 (two-tailed unpaired t-test with Welch's correction). (B) Representative immunostaining (red) for mitosis marker phospho-histone H3 (PH3) for WT and S252W SSCs (Scale bar = 20 μm) and quantification with percentage of PH3-positive cells. Data represent mean ± SD in 5 image fields/genotype (>900 total cells). (C) FACS showing proportions of cell death in trypsinized WT and S252W SSCs stained with propidium iodide (PI). Ethanol-treated SSCs were used as positive control. (D) Cell adhesion to laminin in the presence of growth factors of WT and S252W SSC lines (mean ± SD of three experiments (*i.e.*, different cell lines) with n=3 wells/ experiment. **(**E) Representative QPCR showing changes in expression of differentiation or self-renewal markers in WT and S252W SSC lines after treatment with retinoic acid (RA) for 48 hr (fold change *vs.* vehicle control). Data are mean ± SD (n=3 wells). (F) QPCR showing mean relative *Etv5* expression (± SD; n=4 independent cell lines) in S252W *vs.* WT SSCs. *p< 0.05 (two-tailed, Mann Whitney test). (G-H) QPCR: Relative expression levels (mean ± SD; n=3 wells) for SSC self-renewal and differentiation markers in S252W *vs.* WT SSC lines. Panels A-C, E, G, and H show one out of ≥ two representative experiments performed with independent lines.

Figure S2

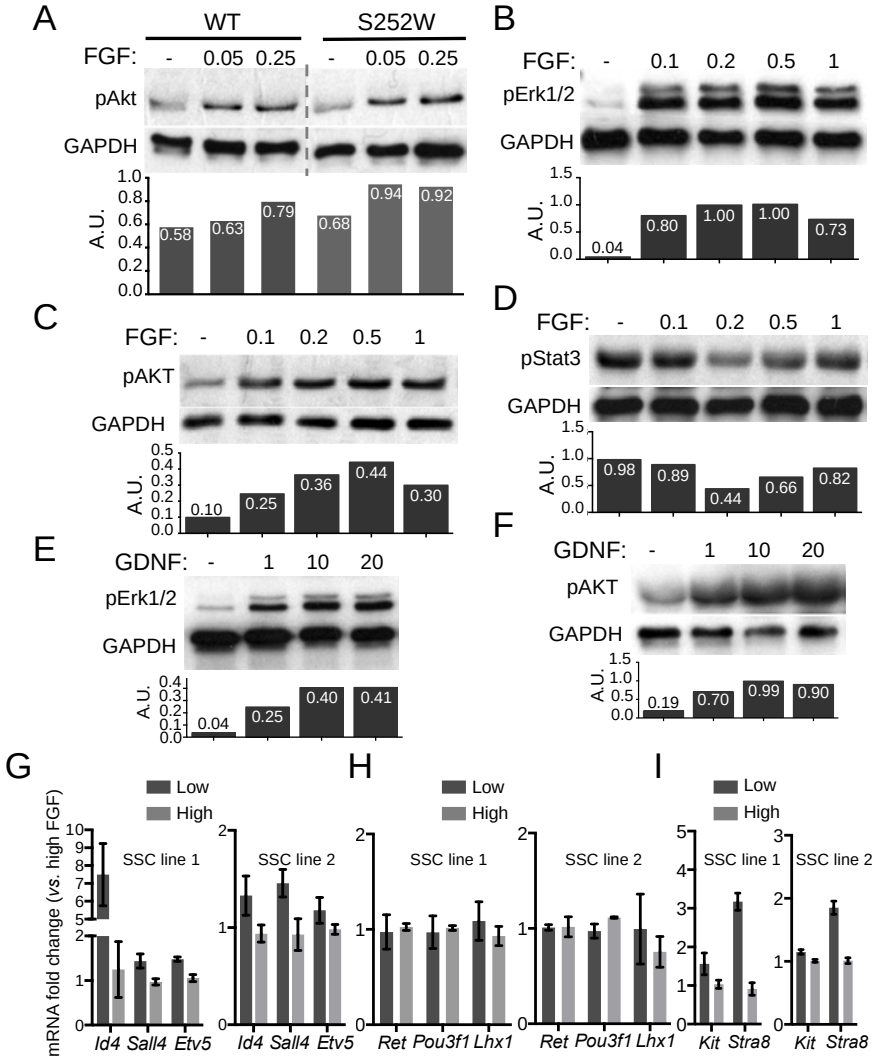

Figure S2, Related to Figure 3. Growth factor dose modulates downstream signaling and expression of self-renewal markers in SSCs. (A) Representative anti-AKT phospho-serine 473 IB in WT and S252W SSCs in response to FGF2 (0.05 and 0.25 ng/ml) after starvation for 16 hr. Grey dashed line denotes a cropped lane. Graphs correspond to densitometric analyses of IB images above each plot for pAkt normalized to loading control (GADPH). Numbers correspond to the quantification for each condition in arbitrary units (A.U.). (B-D) IB and densitometry for changes in pMAPK (*i.e*. pErk1/2), pAKT, and pStat3 in native SSCs (*i.e.,* without hFGFR2) treated with different doses of FGF2 (0-1 ng/ml). (E-F) IB and densitometry for changes in pMAPK (*i.e*. pErk1/2) and pAKT in native SSCs (*i.e.,* without hFGFR2) treated with different doses of GDNF (0-20 ng/ml). Densitometry is normalized to GAPDH. (G-I) QPCR in native SSCs (*i.e.,* without hFGFR2), comparing expression levels of self-renewal and differentiation markers in the presence of FGF2 at low (0.5 ng/ml) *vs* high (10 ng/ml) levels for 1 week in feeder-free conditions. Left and right graphs in each panel correspond to two biological replicates out of ≥2 independent experiments with different SSC lines. Data points represent mean±SD; n=3 technical replicates. (G) Differentially expressed stem cell markers. (H) Stably expressed stem cell markers. (I) Differentiation markers.

Figure S3

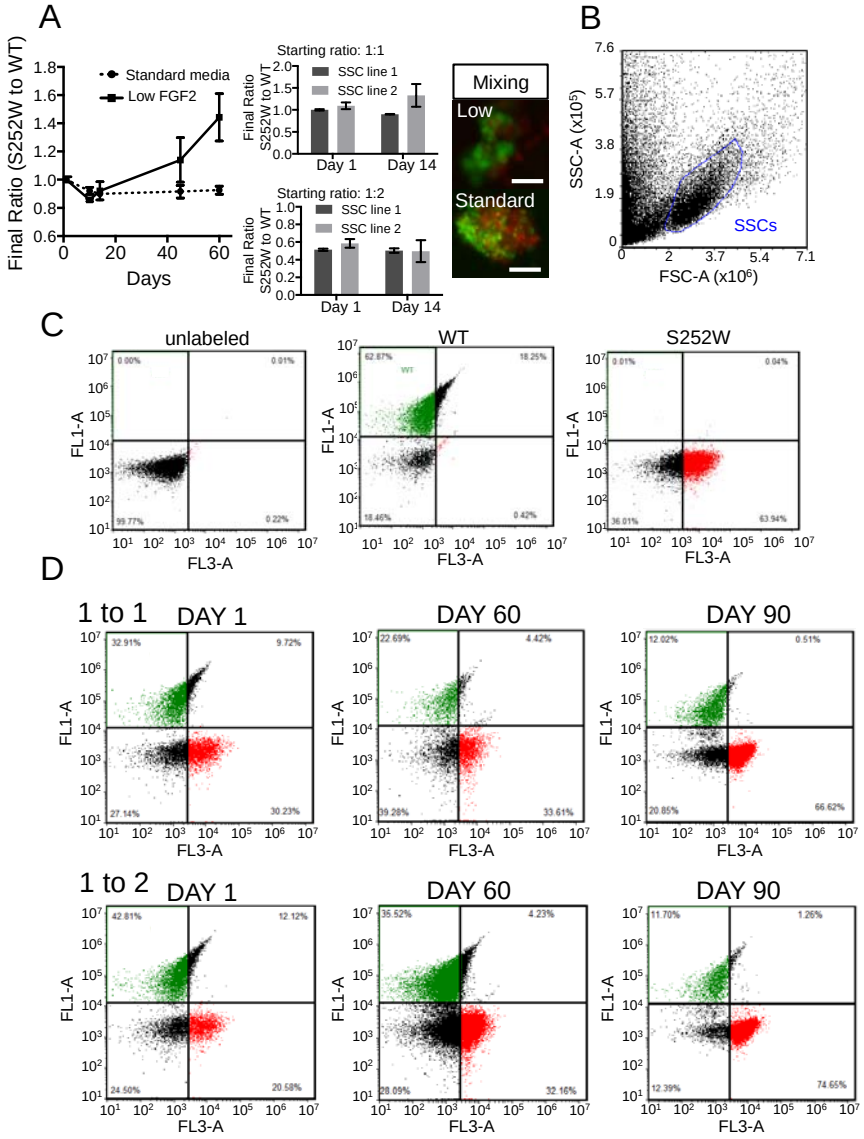

Figure S3, Related to Figure 4. *In vitro* competition assay with representative flow cytometry used for quantification. (A) Left: *In vitro* mixing experiment showing change in ratio (FACS analysis) over time of S252W to WT in standard media or low FGF2 (1 ng/ml). Mutant and WT SSCs were mixed at a 1:1 ratio. Data are from one of two biological replicates (*i.e.*, independent lines), showing the mean±SD (n=3 wells/condition) for each time point. Middle: Bar graphs show results of mixing experiments at day 1 and 2 weeks for 2 independent biological replicates in standard media in both 1:1 (top) and 1:2 (bottom) starting mixing ratios. Error bars correspond to mean±SD (n=3 wells/condition). Right: Fluorescent images correspond to mixed SSC colonies in each condition (scale bar =50 μm) (B-D) Representative FACS data. (B) SSC population (blue) based on forward-scatter (FSC-A) *vs.* side-scatter (SSC-A). (C) Dot plots with quadrants of gated SSCs showing percentage of GFP^+ (green) and $mCherry^+$ (red) SSCs in unlabeled (left), WT (center) and S252W (right) SSC lines cultured in separate wells. (D) Dot plots with quadrants of gated SSCs, showing the percentages of WT-GFP^+ (green) and S252W-$mCherry^+$ (red) SSCs in mixing experiments at different time points for 1:1 (Top) and 1:2 (Bottom) mutant:WT ratios.

Supplemental Experimental Procedures

SSC Lines and Cell Culture

Cell culture media consisted of StemPro-34 (Gibco Cat. No 10640) with nutrient supplement (Gibco Cat No 10641) containing additional supplements and growth factors at the following concentrations: 20 ng/ml GDNF, 10 ng/ml FGF2, 25 μg/ml insulin, and 20 ng/ml EGF. Media changes and culture passages were performed as described previously (Martin and Seandel, 2013). SSC lines stably expressing hFGFR2 alleles driven by the human PGK promoter were generated by lentivirus delivery. Labeling was performed by co-transduction with EGFP or mCherry and hFGFR2 lentivirus. The ratio of EGFP (or mCherry) to FGFR2 was 1:4 by volume. Alternatively, we used pre-labeled SSCs that had been sorted to homogeneity using a BD FACSAria II. Supernatants from 293T cells containing lentiviruses were titrated using p24 ELISA (Lenti-X p24 Rapid Titer Kit, Clontech). Feeder-free SSC cultures were infected with lentivirus over night in SSC media containing polybrene (5 μg/ml). Transduction efficiency was monitored by fluorescence microscopy and by QPCR with specific primers for human FGFR2. FGFR2 protein was detected by immunofluorescence and immunoprecipitation followed by immunoblot as described below. For propidium iodide staining, SSCs were triturated to detach from feeders, trypsinized, treated with 0.5 mg/ml of DNAse I and resuspended in PBS/ 0.1 % bovine serum albumin. Propidium iodide (Calbiochem) was added at 10 μg/ml for 15 min at room temperature, and positive cells were quantified using a BD Accuri C6 Flow Cytometer. Adhesion assays were performed in laminin coated 24-wells (8μg/well overnight at room temperature, Millipore) in the absence of feeders. Specifically, SSCs were triturated off feeders, trypsinized, treated with 0.5 mg/ml of

DNAse I and plated in triplicate at $1x10^3$ cells/mm^2 in standard SSC culture media. Floating and adhered cells were collected two hours after plating and trypsinized prior counting. For co-culture experiments, differentially labeled WT and S252W SSCs were mixed in triplicate wells (at 1:1 or 2:1 WT to S252W ratios) and co-cultured for several weeks *in vitro* in standard cell culture conditions at different FGF2 doses (0.2, 1, and 10 ng/ml). The S252W to WT ratio was measured the day after plating by flow cytometry (BD Accuri C6) and weekly thereafter. Mixed cells were re-plated onto fresh feeders for continuous co-culture.

Retinoic Acid and Growth Factor Treatments

SSCs were plated in gelatin-coated wells without feeders at 2-3 $x10^3$ cells/mm^2 in growth media for retinoic acid (RA) treatment or in starvation media for 12-16 hr. Starvation media consisted of growth media without growth factors (*i.e*. lacking GDNF, FGF2, insulin and EGF) Next, RA or vehicle control (DMSO) was added to 1 μM or 0.5% final concentration, respectively, every 24h for 2 or 3 days. Alternatively, growth factor stimulation was performed for 20 minutes at 37°C in starvation media containing the appropriate growth factor at indicated concentrations.

SSC Transplantation

For *in vivo* evaluation of stem cell activity, differentially labeled WT and S252W SSCs were mixed prior transplantation into host mice or mixed for *in vitro* co-culture for 3 weeks prior to transplantation. SSC transplants were performed as described previously (Seandel et al., 2007). Briefly, adult C57Bl6 male mice at 6-8 weeks of age were treated

with busulfan (40 mg/kg body weight) and used 4-6 weeks later as recipients. SSCs were dissociated with 0.05% trypsin/EDTA, treated with 1 mg/ml DNAse I, and resuspended at a concentration of 8-10 $x10^6$ cells/ml in culture medium containing DNase I and sterile-filtered trypan blue. 10 μl of donor cell suspension was transplanted into each testis by microinjection into the efferent ducts. Two months after transplantation, detunicated recipient testes were analyzed using a fluorescent stereoscope (Zeiss) for the number of GFP or mCherry colonies. Pooled data of transplanted testis included 10 experiments using four independent cell lines at "1 to 1" or "1 to 2" (S252W to WT ratio) in which each genotype was labeled with either GFP or mCherry. For depiction of pooled data, we first normalized the colony number based on the ratio injected. The data were depicted as the percentage of normalized colony numbers for each genotype out of the total. Statistical analyses were performed using GraphPad™.

Immunohistochemistry and Immunofluorescence

Human cadaver testes were obtained from the New York Organ Donor Network. Slides prepared from Bouin's fixed paraffin embedded testis tissue were used for endogenous FGFR2 immunohistochemistry (IHC). Slides were rinsed in xylenes and EtOH to deparaffinize and rehydrate respectively. Next, slides were incubated for 30 min in steamer in Tris-EDTA pH 9 antigen retrieval buffer, cooled for 15 min and incubated in 3% H_2O_2 for 3 min. Slides were blocked with tyramide blocking buffer (TBB; Jacobs et al., 1998) for 30 min and incubated with mouse monoclonal anti-human FGFR2 antibody ([3F8] ab119237, Abcam; 0.1 μg/ml) or control mouse IgG (Jackson ImmunoResearch at 0.1 μg/ml) in TBB over night at 4° C. Slides were then incubated with streptavidin HRP

for 30 min at room temperature (Jackson Immunoresearch 016-030-084 0.5 μg/ml) followed by biotinyl tyramide for 15 min at room temperature (1:200 in PBS with 0.03% H_2O_2). Finally, slides were incubated with streptavidin HRP for 30 min at room temperature and developed for 2.5 min with 0.05% AEC (3-amino-9-ethylcarbazole, Amresco) and 0.015% H_2O_2 in acetate buffer pH 5.5. Hematoxylin was used as the counterstain. For immunofluorescence on cultured cells, SSCs were triturated off from feeders, trypsinized, treated with 1 mg/ml DNAse I and resuspended in growth media. The cell suspension was dried on to glass slides and fixed in 4% PFA for 10 min at room temperature. Cells were blocked using 10% donkey serum before incubation with primary antibodies overnight at 4° C. The following primary antibodies were used: mouse monoclonal anti-human FGFR2 antibodies ([3F8] ab119237, Abcam; and Bek (C-8) sc-6930, Santa Cruz Biotechnology) and anti-phospho-Histone H3 (Ser10) antibody (Millipore 06-570). Detection of primary antibodies was performed with biotin-conjugated secondary antibodies followed by Alexa488-conjugated streptavidin. Slides were counterstained and mounted with ProLong Gold antifade reagent (Invitrogen) and analyzed using Olympus BX50 microscope. For phospho-H3 quantification, images were captured from multiple randomly selected areas counting >900 cells in total for each cell line. Total cell number per area was determined by counting DAPI-stained nuclei, followed by quantification of pH3 positive cells. IH and IF images were captured with Olympus BX50 fluorescence microscope.

Immunoprecipitation and Immunoblot

Feeder-free SSCs were suspended in lysis buffer containing PMSF (Sigma) and protease and phosphatase inhibitors cocktails (Sigma). For immunoprecipitation, 75 μg of protein lysate was incubated overnight at 4° C with anti-human FGFR2 rabbit monoclonal antibody (D4H9, Cell Signaling) followed by incubation with protein A agarose beads for 3 hr at 4° C. Immunocomplexes were washed three times with lysis buffer, and the pellet was resuspended in 2x Laemmli sample buffer, separated by SDS-PAGE, and transferred to a PVDF membrane (Amershan) for detection with mouse monoclonal anti-human FGFR2 antibody ([3F8] ab119237, Abcam) as described next. Immunoblot was performed following standard procedures. Briefly, 10 to 15 μg of total cell lysates were separated by SDS-PAGE and transferred into PVDF membrane (Amershan). Membranes were blocked in Tris-buffered saline containing 0.1% Tween-20 (TBST) with 3% BSA and incubated with the following primary antibodies: anti-pAkt (Ser473, Cell Signaling), anti-pAkt (Ser473, R&D Systems), anti-p44/42 MAP Kinase (Cell Signaling), and anti phosphoStat3 (Tyr705) (clone M9C6, Cell Signaling). Anti-GAPDH (mouse monoclonal, Abcam) was used as a loading control. Blots were washed with TBST and incubated at room temperature with the appropriate secondary antibody conjugated to horseradish peroxidase. Chemiluminescent immunodetection was performed with ECL system (Amersham), and membranes were exposed to X-ray film (Hyperfilm ECL, Amersham). Digitized scans of the blots were analyzed using ImageJ for densitometry.

Reverse Transcription Polymerase Chain Reaction (RT-PCR) and Quantitative Reverse Transcription Polymerase Chain Reaction (QPCR)

Total RNA was extracted from snap-frozen human cadaver testis samples or feeder-free cultured SSCs using RNeasy Plus extraction kit (Qiagen). RNA was reverse transcribed using qScript cDNA SuperMix (Quanta Biosciences). PCR amplification was performed with Platinum Taq Polymerase. QPCR was performed in a LightCycler 480II real-time System (Roche) with PerfeCta SYBR Green FastMix (Quanta Biosciences). For quantification, data was normalized to endogenous β-actin and GAPDH and relative transcript expression was calculated using the comparative C_T method ($2^{-\Delta\Delta Ct}$ method).

Molecular Biology

Human FGFR2 cDNA was obtained from GeneCopoeia (clone A0979, catalog no EX-A0979-M02) and used as template to generate the hFGFR2 S252W mutant cDNA using QuikChange II Site-Directed Mutagenesis Kit (Agilent Technologies) according to the manufacturer's protocol. The mutagenesis primers were fwd 5'-TGTTGTGGAGCGATG GCCTCACCGGC-3' and rev 5'-GCCGGTGAGGCCATCGCTCCACAACA-3'. WT and S252W expression vectors for lentivirus production were prepared as follows: full-length WT and S252W cDNAs were amplified using primers containing BamHI and SalI restriction sites at the 5' and 3' end of the PCR product respectively (fwd 5'-CGCGG ATCCACCATGGTCAGCTGGGGTCGTTTC-3' and rev 5'-GCCGACGTCGACTCAT GTTTTAACACTGCCGTTTATG-3'). Digested PCR products were subcloned into pCCL4-PGK expression vector using BamHI and SalI sites. The final constructs were sequenced in the Applied Biosystems Automated 3730xl DNA Analyzer.

Statistics

Results are presented as means ± SD. The number of independent biological or technical replicates is indicated by "n". The statistical significance was determined by two-tailed unpaired t-test, Wilcoxon matched-pairs signed rank test, or the Kruskal-Wallis test as indicated in each figure (GraphPad Prism, version 6.0). Results were considered significant at p-value < 0.05 ($p < 0.05$ is indicated as *; $p < 0.005$ is indicated as ***). NS = not significant.

Primer Sequences for QPCR

Human *FGFR2*
Fwd.1 5'-TGACACCGATGGTGCGGAAGA-3'
Rev.1 5'-CGGCTGGGCAGCGAAACTTG-3'
Fwd.2 5'-GAATATCATAAATCTTCTTGGAGC-3'
Rev.2 5'-TCATAGGAGTACTCCATCCCG-3'
Mouse *Fgfr2*
Fwd.1 5'-TCCAACGCCCACAATGAGGTG-3'
Rev.1 5'-CTGACGGGACCACACTTTCC-3'
Fwd.2 5'-GTCTGTCCTCAACAGCGGAC-3'
Rev.2 5'-CCCACTGCTTCAGCCATGAC-3'
Mouse *Etv5*
Fwd 5'-AGAACCTGGATCACAGCAAC-3'
Rev 5'-ACTATCTCCAGGAACTCCTG-3'
Mouse *Stra8*
Fwd 5'-TCCCAGTCTGATATCACAGC-***3***
Rev 5'-TCCCATCTTGCAGGTTGAAGG-3'
Mouse kit
Fwd 5'- GCCAGTGCTTCCGTGACATT-3'
Rev 5'- TGCCATTTATGAGCCTGTCGTA-3'
Mouse Ret
Fwd 5'- GGCTGTCCCGAGATGTTTATG-3'
Rev 5'- GACTCAATTGCCATCCACTTGA-3'
Mouse P*ou5f1*
Fwd *5'*-AGCAACTCAGAGGGAACCTCC-*3*'

Rev 5’-GGTGATCCTCTTCTGCTTCAG-3’

Mouse *Plzf*

Fwd 5’- TTTGCGACTGAGAATGCATTTAC-3’

Rev 5’-ACCGCATTGATCACACACAAAG-3’

Mouse *Id4*

Fwd 5’-ACTACATCCTGGACCTGCAG-3’

Rev 5’-TGCTGTCACCCTGCTTGTTC-3’

Mouse *Sall4*

Fwd 5’-AGCACTGC TGCACACGGTGTG-3’

Rev 5’- GTCATGTAGTGTACCTTCAGG-3’.

Mouse *Lhx1*

Fwd 5’-AAGCCAAGCAACTGGAGACG- 3’

Rev 5’- GATTCTGGAACCAGACCTGG-3’

Mouse *Pou3f1*

Fwd 5’-AAGCAACGACGCATCAAG C-3’

Rev 5’-TTGCACATGTTCTTGAAGCTC-3’

Mouse *Itga6*

Fwd 5’-CTGCAGCGTCAACGTGAGGTGT-3’

Rev 5’-ACTCGAACCTGAGTGCCCGC-3’

Mouse *Gfrα1*

Fwrd 5’- AGCAACAGTGGCAATGACCTG -3’

Rev 5’- AGTGGTAGTCGTGGCAGTGG -3’

Mouse *p21*

Fwd 5′-GCAGATCCACAGCGATATCC-3′

Rev 5′-CAACTGCTCACTGTCCACGG-3′

Mouse *p27*

Fwd 5’ GGGTTAGCGGAGCAGTGTCC 3’

Rev 5’ GTCTGCTCCACAGTGCCAGC 3’

Supplemental References

Jacobs, W., Dhaene, K., and Van Marck, E. (1998). Tyramine-amplified immunohistochemical testing using "homemade" biotinylated tyramine is highly sensitive and cost-effective. Archives of pathology & laboratory medicine *122*, 642-643.